Definition and Use of the Experimental Sensible Parameters To Characterize Sensitivity and Precision of a Generic Oxygen Optical Sensor

ARTICLE *in* ANALYTICAL CHEMISTRY · JUNE 2008

Impact Factor: 5.64 · DOI: 10.1021/ac800551a · Source: PubMed

Anal. Chem. **2008,** *80,* 2091−2096

Definition and Use of the Experimental Sensible Parameters To Characterize Sensitivity and Precision of a Generic Oxygen Optical Sensor

Denis Badocco and Paolo Pastore*

Department of Chemical Sciences, University of Padua, Via Marzolo 1, 35131 Padua, Italy

Experimental data, obtained with an oxygen optical sensor constituted by a polysulfone layer embedding ruthenium(II)(4,7-diphenyl-l,l0-phenanthroline)octylsulfate (Ru(dpp)OS), were rationalized by using the digital simulation technique and generalized for different sensors. The experimental, asymmetric, emission shape was used to define two sensible parameters, ASY (asymmetry factor) and $\Delta I_{\%}$ (percent variation of emission intensity), to characterize the sensitivity of a generic oxygen optical sensor (represented by the Stern−Volmer constant, K'_{SV}). Correlations between ASY and K'_{SV} and between $\Delta I_{\%}$ and K'_{SV} were established, and a double working curve was proposed to evaluate with a single light emission measurement the K'_{SV} value with the best precision. Sensitive membranes ($-\log K'_{SV} = pK'_{SV} < 0.5$) had high precision only for low $\%O_2$ values; poorly sensitive membrane ($pK'_{SV} > 2.5$) had constant but scarce precisions in a large $\%O_2$ interval. For $\%O_2$ up to 21% (air) good values are $pK'_{SV} = 0.5-1.0$. In order to monitor a wider $\%O_2$ range, $pK'_{SV} = 1.5-2.0$ are good choices. A simple mathematical model allowed one to estimate the oxygen diffusion coefficient inside the layer, D_{O_2}, and its solubility in the polymer matrix, s_{O_2}, from the simple measurement of the membrane thickness, response time, t_{90}, and luminescence lifetime. $D_{O_2} = 2 \times 10^{-8}$ cm^2 s^{-1} and $s_{O_2} = 2.2 \times 10^{-3}$ mol atm^{-1} cm^{-3} were estimated for our membranes. The proposed working curves gave very good results even with literature data.

Optical sensors are revolutionizing the determination of molecular oxygen both in gas mixtures and in water.[1,2] The determination of oxygen concentration is important in many areas of industry, medicine, and the environment. Optical sensors are more attractive than conventional amperometric devices because, in general, they eliminate the need of frequent membrane replacement due to poisoning, stirring, and of frequent calibration during deployments, have a fast response time, and do not consume oxygen. They utilize luminescence quenching of suitable luminophors in the presence of oxygen. Typical luminophors are transition metal complexes with phenanthrolines,[3,4] porphyrins,[5,6] and bipyridines.[7−10] They are entrapped in thin layer films constituted by sol−gel,[1] polymer,[1,4,6,11] or hybrid materials.[5,12−14] The continuous development of these devices fully justifies theoretical studies dedicated to the knowledge of the parameters affecting both signal and chemical/physical properties of the sensors together with the searching of test parameters able to characterize the sensing layers. In particular, the starting point is the following general quenching scheme:

$$M + h\nu \rightarrow M^* \quad k_{abs} \tag{1}$$

$$M^* \rightarrow M + h\nu' \quad k_f^0 \tag{2}$$

$$M^* \rightarrow M + \text{heat} \quad k_i \tag{3}$$

$$M^* + Q \rightarrow M + Q \quad k_q \tag{4}$$

$$M^* + M \rightarrow M + M \quad k_{sq} \tag{5}$$

In this scheme M, M*, and Q are the luminescent molecule at the fundamental state , the luminescent molecule at the excited state, and the quencher species, respectively; $h\nu$ and $h\nu'$ are the photon energies absorbed and emitted; k_{abs}, k_f^0 are the absorption and emission rate constants; k_i represents all the nonradiative decays; k_q, k_{sq} are the quenching and the self-quenching rate constants. According to the steady state theory the luminescence quantum yield, Φ_l, is given by

* Corresponding author.

(1) Ando, M. *Trends Anal. Chem.*, **2006**, *25*, 937.
(2) Amao, Y. *Microchim. Acta* **2003**, *143*, 1.
(3) König, B.; Kohls, O.; Holst, G.; Glud, R. N.; Kühl, M. *Mar. Chem.* **2005**, *97*, 262.
(4) Florescu, M.; Katerkamp, A. *Sens. Actuators, B* **2004**, *97*, 39.
(5) Lu, X.; Manners, I.; Winnik, M. A. *Macromolecules* **2001**, *34*, 1917.
(6) Gulino, A.; Giuffrida, S.; Mineo, P.; Purrazzo, M.; Scamporrino, E.; Ventimiglia, G.; Van der Boom, M. E.; Fragala, I. *J. Phys. Chem. B* **2006**, *110*, 16781.
(7) Fuller, Z. J.; Bare, W. D.; Kneas, K. A.; Xu, W.-Y.; Demas, J. N.; DeGraff, B. A. *Anal. Chem.* **2003**, *75*, 2670.
(8) Ramamoorthy, R.; Dutta, P. K.; Akbar, S. A. *J. Mater. Sci.* **2003**, *38*, 4271.
(9) Xiong, X.; Xiao, D.; Choi, M. M. F. *Sens. Actuators, B* **2006**, *117*, 172.
(10) Sohmiya, M.; Sugahara, Y.; Ogawa, M. *J. Phys. Chem. B* **2007**, *111*, 8836.
(11) Vasylevska, G. S.; Borisov, S. M.; Krause, C.; Wolfbeis, O. S. *Chem. Mater.* **2006**, *18*, 4609.
(12) McDonagh, C.; Bowe, P.; Mongey, K.; MacCraith, B. D. *J. Non-Cryst. Solids* **2002**, *306*, 138.
(13) MacCraith, B. D.; McDonagh, C. *J. Fluoresc.* **2002**, *12*, 333.
(14) Tang, Y.; Tehan, E. C.; Tao, Z.; Bright, F. V. *Anal. Chem.* **2003**, *75*, 2407.

10.1021/ac702202t CCC: $40.75
Published on Web 02/15/2008

$$\Phi_l = \frac{k_f^0}{k_f^0 + \sum k_i + k_{sq}[M] + k_q[Q]} \quad (6)$$

In the absence of Q and at low M concentration

$$\Phi_l^0 = \frac{k_f^0}{k_f^0 + \sum k_i} \quad (7)$$

Defining $\tau_0 = \{1\}/\{k_f^0 + \Sigma k_i\}$ as the luminescence lifetime in the absence of quencher, the ratio between eq 7 and 6 and gives the Stern−Volmer equation:[15,16]

$$\frac{\Phi_l^0}{\Phi_l} = 1 + \frac{1}{k_f^0 + \sum k_i} k_q[Q] = 1 + \tau_0 k_q[Q] = 1 + K_{SV}[Q] \quad (8)$$

The ratio $(\Phi_l^0)/(\Phi_l)$ may be experimentally determined both by I^0/I and τ_0/τ. According to Henry's law, the oxygen concentration inside the membrane is proportional to p_{O_2}

$$[O_2] = s_{O_2} p_{O_2} \quad (9)$$

s_{O_2} being the oxygen solubility in the polymer. If the quenching reaction is diffusion controlled, then k_q is proportional to the oxygen diffusion rate constant, k_d according to

$$k_q = \alpha k_d \quad (10)$$

where α is the quenching probability. From the Smoluchowski equation

$$k_q = \alpha \frac{4\pi N \sigma D}{1000} \quad (11)$$

where N is Avogadro's number, σ is the collision radius, and D ($D_{Ru} + D_{O_2}$), approximated to D_{O_2}, is the diffusion coefficient of oxygen into the polymer. The Stern−Volmer equation becomes

$$\frac{I^0}{I} = 1 + \alpha \frac{4\pi N \sigma}{1000} \tau_0 D_{O_2} s_{O_2} p_{O_2} \quad (12)$$

Converting the oxygen partial pressure to percent molar fraction, $\%O_2$, we obtain

$$\frac{I^0}{I} - 1 = \alpha \frac{4\pi N \sigma P_{tot}}{10^5} \tau_0 D_{O_2} s_{O_2} \%O_2 = K'_{SV} \%\, O_2 \quad (13)$$

From these theoretical considerations, it is evident that the key parameters for understanding the response of the system to the presence of oxygen (assuming diffusion controlled quenching and constant pressure and temperature) are the unquenched lifetime of the dye (τ_0), the oxygen diffusion coefficient inside the layer (D_{O_2}), and the solubility (s_{O_2}) of oxygen in the polymer matrix.

In this paper, experimental data, obtained with an oxygen optical sensor constituted by a polysulfone layer embedding a luminescent dye (ruthenium(II)(4,7-diphenyl-l,l0-phenanthroline)-octylsulfate, Ru(dpp)OS), will be rationalized by using the digital simulation technique. In particular, working curves will be proposed to test the sensing layers, allowing the determination of the membrane sensitivity represented by the Stern−Volmer constant, K'_{SV}, with a single measurement. The working curves will be described by the percent variation of the emission intensity, $\Delta I_{\%}$, and by the asymmetry factor, ASY, resulting from the experimental emission when oxygen gets into and exits the sensing layer. From this result, with suitable mathematical models, other characteristic parameters of the membrane will be determined, namely, the oxygen diffusion coefficient inside the layer, D_{O_2}, and the oxygen solubility in the polymer matrix, s_{O_2}. The only experimental requirement will be the measurement of the luminescence lifetime and the membrane response time, t_{90}. The working curves will be successfully used also for the evaluation of different membranes and dyes whose behavior has been already described in the literature.

EXPERIMENTAL SECTION

Reagents. Ruthenium(III) chloride trihydrate (99.98%), and 4,7-diphenyl-l,l0-phenanthroline (dpp), sodium octyl sulfate (Na-OS), $CHCl_3$ anhydrous ≥99%, $CHCl_3$ (99%), polysulfone d = 1.24 g/L, M_n, 16 000, M_w, 35 000, were obtained from Aldrich Products. Ultrapure water was obtained with a Millipore Plus System (Milan, Italy, resistivity 18.2 MΩ cm^{-1}).

Procedures. Ru(dpp)OS was synthesized according to ref 17.

Preparation of Oxygen-Sensitive Membranes. The polysulfone membranes investigated were prepared by dip coating onto a glass support (10 mm × 30 mm × 1 mm). Glass was previously washed with water and soap, rinsed with water, then rinsed with isopropanol, and dried under nitrogen flow. Membranes were obtained dissolving a suitable amount of the ruthenium complex and polysulfone in dry chloroform.

Apparatus. *Oxygen Optical Sensor.* The oxygen sensor built in our laboratory is essentially constituted of the oxygen sensitive membrane deposited on a glass support; a high-brightness blue excitation LED (Nichia, NSPE590, angle 15°, λ_{max} = 464 nm) normal to the membrane surface and shielded with a Kodak (no. 21 Kodak wratten gelatin filter) long-wave-pass gel filter (cutoff 570 nm) were used; emission light was focused onto a Hammamatsu S1223 photodiode detector (Hamamatsu, Middlesex, U.K.).

Oxygen and nitrogen were mixed and flowed via mass flow controllers into the sensor cell. The signal output was directed to a LeCroy Wave Surfer 44xs, 450 MHz, oscilloscope (Geneva,

(15) Fernàndez-Sànchez, J. F.; Cannas, R.; Spichiger, S.; Steiger, R.; Spichiger-Keller, U. E. *Anal. Chim. Acta* **2006**, *566*, 271.

(16) McDonag, C.; Kolle, C.; McEvoy, A. K.; Dowling, D. L.; Cafolla, A. A.; Cullen, S. J.; MacCraith, B. D. *Sens. Actuators, B* **2001**, *74*, 124.

(17) Klimant, I.; Wolfbeis, O. S. *Anal. Chem.* **1995**, *67*, 3160.

Switzerland). Lifetimes were determined from pulsed irradiation realized with a Thurby Thandar Instruments TGP110 pulse generator. Gas mixtures were prepared by mixing suitable amounts of nitrogen and oxygen. The exact composition was determined after mixing with a commercial, calibrated oxygen sensor, PBI Dansensor O_2 (Milan, Italy). A Perkin-Elmer lambda 25 UV−vis spectrophotometer was used to determine the thin layer thickness.

Simulation Model. The model describing the oxygen/nitrogen diffusion inside a porous membrane of thickness, L, refers to Fick's second law in one geometric dimension

$$\frac{\partial u}{\partial t} = D_R \frac{\partial^2 u}{\partial x^2} \tag{14}$$

In this equation u is the concentration in terms of oxygen percentage. It is a function of time, t, and distance, x. With the fully explicit Euler method, Fick's seond law is expressed as

$$\frac{u_{i,j+1} - u_{i,j}}{\Delta t} \cong D_{O_2} \frac{u_{i-1,j} - 2u_{i,j} + u_{i+1,j}}{\Delta x^2} \tag{15}$$

where i and j indicate subsequent time space grid positions where the concentrations are defined. Temporal and spatial increments and the diffusion coefficient are given by Δt, Δx, and D_{O_2}, respectively. Developing the system in the space grid, we obtain the algorithm in matricial form

$$U_{j+1} \cong AU_j + \lambda V_j, \quad j = 0,1,....N-1 \tag{16}$$

where $\lambda = D_{O_2}(\Delta t)/(\Delta x^2)$ and A is the following trigonal matrix:

$$A = \begin{pmatrix} 1-2\lambda & \lambda & 0 & \cdots & 0 & 0 \\ \lambda & 1-2\lambda & \lambda & \cdots & 0 & 0 \\ 0 & \lambda & 1-2\lambda & \cdots & 0 & 0 \\ \cdots & \cdots & \cdots & \cdots\cdots & & \cdots \\ 0 & 0 & 0 & \cdots & 1-2\lambda & \lambda \\ 0 & 0 & 0 & \cdots & \lambda & 1-2\lambda \end{pmatrix} \tag{17}$$

U_j and V_j are vectors containing the dimensional concentrations and boundary condition, respectively:

$$U_j = (u_{1,j}, u_{2,j}, \ldots, u_{N-1,j})^T \tag{18}$$

$$V_j = (u_{0,j}, 0, \ldots, 0, u_{N,j})^T \tag{19}$$

As usual for explicit methods, the stability condition is $\lambda \leq 1/2$. The boundary conditions define the geometric characteristics of the layer (in particular the thickness, L) and the diffusion conditions of oxygen. Initial conditions are the following

$$t = 0 \quad u_{0,0} = 100, \quad u_{i,0} = 0, \quad i = 1,2,...N$$

When oxygen permeates the membrane from the outside

$$t > 0 \begin{cases} i = 0 & u_{0,j} = 100 \\ i = N & u_{N,j} = u_{N-1,j} \end{cases}$$

When oxygen permeates from the membrane to the outside

$$t > 0 \begin{cases} i = 0 & u_{0,j} = 0 \\ i = N & u_{N,j} = u_{N-1,j} \end{cases}$$

Under the following hypothesis the chosen conditions hold: (1) negligible variation of porosity of different matrices, (2) negligible effect of the flow rate (gas flows much more rapidly than diffusion inside the layer), (3) negligible adsorption of O_2 on the matrix, (4) negligible internal filter effect (signal saturation), (5) all the luminophor is available for quenching, and (6) negligible light scattering.

If we imagine the membrane divided into thin layers of thickness Δx, the emitted light in the thin layer is

$$I^0_{i,j} = I^0 \frac{\Delta x}{L} \tag{20}$$

where $I^0_{i,j}$ is the contribution of the ith layer to the total intensity I^0 at the jth iteration time. In the presence of a quencher (oxygen in our case), light emission intensity may be obtained from the SV eq 13 so that, for a single thin layer and for the entire membrane thickness, we can write, respectively,

$$\frac{I^0_{i,j}}{I_{i,j}} = 1 + K'_{SV} u_{i,j} \tag{21}$$

$$I_j = \sum_{i=1}^{N} I_{i,j} = \sum_{i=1}^{N} \frac{I^0_{i,j}}{1 + K'_{SV} u_{i,j}} = \frac{I^0}{L} \sum_{i=1}^{N} \frac{\Delta x}{1 + K'_{SV} u_{i,j}} \tag{22}$$

The simulation, therefore, uses the following dimensionless emission intensity and time variables:

$$\omega_j = \frac{I_j}{I^0} \tag{23}$$

$$\gamma_j = j \frac{\Delta t D_{O_2}}{L^2} \tag{24}$$

RESULTS AND DISCUSSION

Definition of the Sensible Parameters. Figure 1 shows the experimental signal recorded on passing from air (21% oxygen and 79% N_2) to pure nitrogen and back to air. Signal repeatability is very good so that the same difference of intensity is always observed. From the emission intensity variation, caused by quenching effects, it is possible to define the parameter $\Delta I_{\%}$

$$\Delta I_{\%} = \frac{\Delta I}{I^0} \times 100 \tag{25}$$

It must be noted that, owing to the chosen normalization, $\Delta I_{\%}$ is equivalent to the theoretical $\Delta\omega_{\%} = (I^0 - I_{plateau})/(I^0) \times 100$, where $I_{plateau}$ is the plateau emission value in the presence of a generic oxygen percentage. For this reason we will use $\Delta I_{\%}$ henceforth. From the data in Figure 1 we may also define t_{90} as the time taken to bring the signal from 10 to 90%. It is evident that the time taken

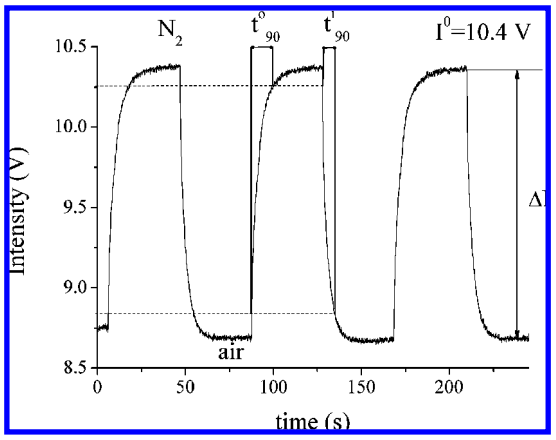

Figure 1. Signal relative to the transition from air (oxygen 21%) to pure nitrogen and return vs time. The membrane was obtained by dip-coating in a mixture containing 20 mmol Ru(dpp)OS and 1 g of (PSF) in 5 mL of $CHCl_3$. Simulation parameters: $N = 25$ (space grid), $\lambda = 0.5$, $\Delta t = \Delta x^2\lambda/D$ for stability condition, $L = 4.3$ μm, $D_{O_2} = 2 \times 10^{-8}$ cm^2/s, $K'_{SV} = 0.01$; total time iteration for a complete cycle, $j_{max} = 10\,816$.

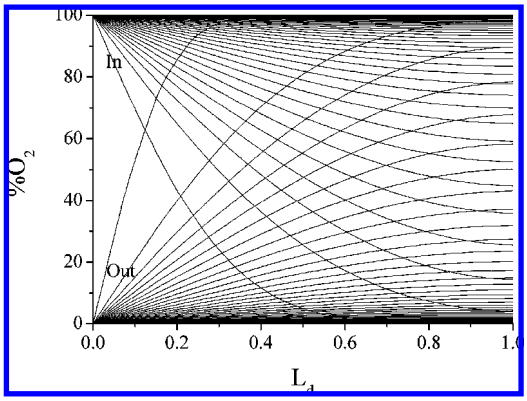

Figure 2. Oxygen concentration profiles vs dimensionless membrane thickness, L_d, during gas permeation through the membrane. Other simulation parameters reported in Figure 1. Concentration profiles reported, 250, relative to regular time intervals.

by oxygen to come out the membrane (t^o_{90}) is longer than that taken to go in (t^i_{90}). This asymmetry may be described by the ASY factor simply defined as

$$\mathrm{ASY} = \frac{t^o_{90}}{t^i_{90}} \qquad (26)$$

Simulation perfectly overlaid the experimental curve so that it was not reported in the plot. It was successfully tested also with experimental data present in the literature,[5] where the sensitive layers were made of different materials. We therefore used simulated data to interpret the experimental ones.

Interpretation of the Emission Shape. The profiles in Figure 2 immediately indicate the natural, unavoidable cause of the observed asymmetry. They represent the concentration profiles of oxygen entering and exiting the polymeric layer. The 0 value of the L_d axis corresponds to the boundary with outside, and $L_d = 1$ corresponds to the junction of the membrane to the glass

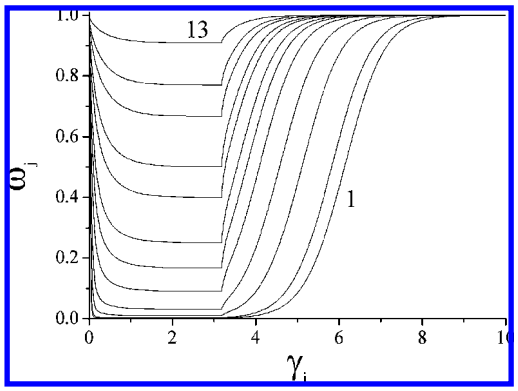

Figure 3. Simulated dimensionless light emission vs dimensionless time on passing from 100% to 0% oxygen. From 1 to 13: $pK'_{SV} = -1.00, -0.70, 0.00, 0.30, 0.52, 1.00, 1.30, 1.52, 1.82, 2.00, 2.30, 2.52, 3.00$. Other simulation parameters as in Figure 1.

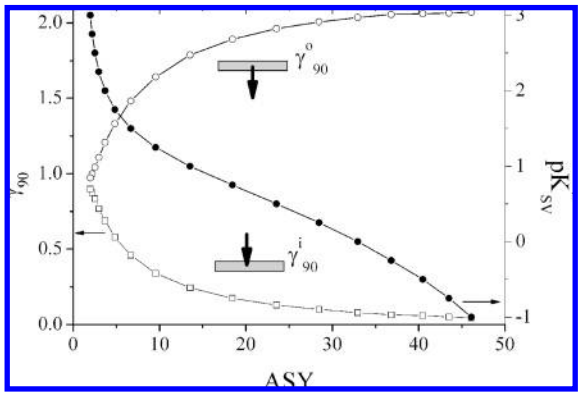

Figure 4. γ_{90} and pK'_{SV} (○, □ and ●, respectively) plotted vs ASY. The symbols are simulated data, and the lines come from the models reported in Table 1. Data refers to oxygen percentage ranging from 0 to 100%. pK'_{SV} values as in Figure 3.

support. The asymmetry, observed also by other authors,[5,18,19] may be easily understood from the asymmetry of the boundary conditions, necessary to describe the phenomenon. During the going in time, oxygen is always 100% (or constant) outside of the membrane and reaches 100% also inside (at $L_d = 1$), but during the coming out period, outside oxygen is 0 and in the inner boundary (the glass support surface) oxygen slowly decreases its amount producing a longer residence time. Because of this diffusive character, the ASY factor depends on D_{O_2}. Moreover, as K'_{SV} is directly proportional to D_{O_2} (see eq 13), ASY and K'_{SV} must be correlated.

Correlation between ASY and K'_{SV}. Figure 3 shows the simulated dimensionless emission profiles vs dimensionless time. The curves correspond to thirteen pK'_{SV} values producing a rising signal (N_2 permeates the membrane) and a decreasing one (O_2 permeates the membrane). From this figure, two facts are evident: (1) the asymmetry increases with K'_{SV} and (2) the $\Delta\omega_{\%}$ (corresponding to the experimental $\Delta I_{\%}$) decreases on increasing K'_{SV}. From these observations we may build the curve represented in Figure 4. It shows the dimensionless γ_{90} (defined

(18) Ruffolo, R.; Evans, C. E. B.; Liu, X.; Ni, Y.; Pang, Z.; Park, P.; McWilliams, A. R.; Gu, X.; Lu, X.; Yekta, A.; Winnik, M. A.; Manners, I. *Anal. Chem.* **2000**, *72*, 1894.
(19) Jayarajah, C. N.; Yekta, A.; Manners, I.; Winnik, M. A. *Macromolecules* **2000**, 33, 5693.

Table 1. Models Representing the Working Curves of t_{90} and pK'_{SV} as a Function of ASY

	$\gamma^{o}_{90} = a_0 \ln(a_1/\mathrm{ASY}^2 + a_2)$	
$pK'_{SV} = a_0 + a_1/\mathrm{ASY} + a_2\mathrm{ASY}^2$	γ^{o}_{90}	γ^{i}_{90}
$\chi^2/(n-3) = 7.8 \times 10^{-4}$	$\chi^2/(n-3) = 1.8 \times 10^{-4}$	$\chi^2/(n-3) = 5 \times 10^{-5}$
$R^2 = 0.9996$	$R^2 = 0.9992$	$R^2 = 0.9996$
$a_0 = 0.869$ (0.017)	$a_0 = -0.2295$ (0.0043)	$a_0 = 0.1904$ (0.0027)
$a_1 = 4.173$ (0.056)	$a_1 = 0.0641$ (0.0066)	$a_1 = 466.8$ (25.1)
$a_2 = -0.00091$ (0.00001)	$a_2 = 0.00008$ (0.00002)	$a_2 = 1.076$ (0.026)

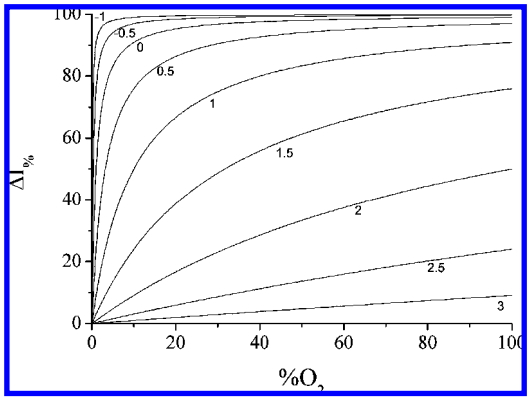

Figure 5. $\Delta I_{\%}$ in logarithmic scale vs $\%O_2$. Each curve was computed with the indicated pK'_{SV} value. pK'_{SV} values as in Figure 3.

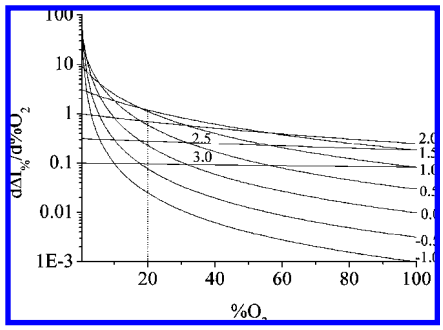

Figure 6. First derivative of the curves in Figure 5, in logarithmic scale, vs $\%O_2$.

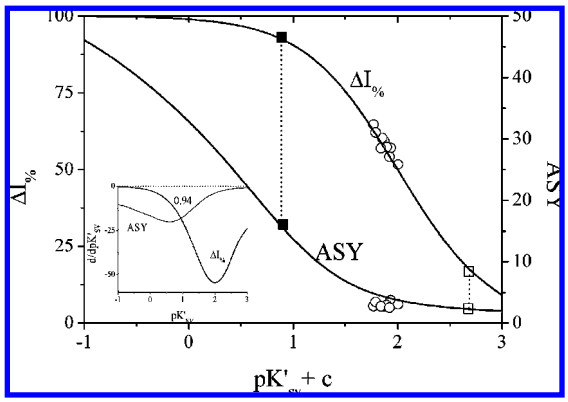

Figure 7. $\Delta I_{\%}$ and ASY vs $pK'_{SV} + c$, (□) membrane of Figure 2 (ASY = 1.87); (■) membrane in ref 5 (ASY = 15); (○) membranes, made by us, characterized by various Ru(dpp)OS concentrations and thicknesses in the range 0.5−10 μm. Theoretical data were obtained from data in Figure 4. Inset, first derivative of the two working curves.

analogously to t_{90}) and pK'_{SV} parameters (○, □ and ●, respectively) plotted vs ASY. It must be pointed out that in this representation, ASY was computed as the ratio between the γ_{90} values. The models describing γ_{90} and pK'_{SV} are the function reported in Table 1. The best fit was obtained by minimizing the statistical parameter χ^2. In this representation, ASY is a very simple parameter to determine the membrane sensitivity. The central part of the plot gives an accurate estimate of K'_{SV} values while the external give lower precision. ASY = 1.9 was obtained with the Ru complex used in this study having $\tau_0 = 6$ μs, while with platinum octaethylporphine ($\tau_0 = 100$ μs), in composite polymer/silica layers,[5] an ASY close to 15 was obtained. The pK'_{SV} values obtained with the working curve are coherent to those experimentally determined with calibration plots (2 in our case and 0.2 in the case of ref 5).

Correlation between $\Delta I_{\%}$ and K'_{SV}. The $\Delta I_{\%}$ parameter is correlated to pK'_{SV} according to eq 13 which may be written as

$$\Delta I_{\%} = \frac{100}{1 + \dfrac{10^{pK_{SV}}}{\%O_2}} \qquad (27)$$

Figure 5 represents eq 27 by plotting $\Delta I_{\%}$ in logarithmic scale vs $\%O_2$. Each curve was computed with the indicated pK'_{SV} value. The curve shape clearly shows that a very sensitive membrane (low pK'_{SV} values) is actually poorly accurate for the determination of large oxygen amounts as $\Delta I_{\%}$ rapidly reaches 100%. On the other hand, poorly sensitive membranes (high pK'_{SV} values) are characterized by low $\Delta I_{\%}$ so that they may detect oxygen from 0 to 100% but with low precision. This is even better evidenced in Figure 6 reporting the first derivative of the curves of the previous figure. The first derivative represents the precision of the measurement. For very sensitive membranes ($pK'_{SV} < 0.5$), precision is very high only for low $\%O_2$ values and rapidly decreases with increasing $\%O_2$; for poorly sensitive membranes ($pK'_{SV} > 2.5$), precision is constant but very low. Consequently, an optical oxygen sensor works best only in limited intervals of $\%O_2$ and it would have to be specifically built for that interval. In other words, the pK'_{SV} value must be suitably chosen for the required precision. This may be done by choosing the suitable luminophor and the characteristics of permeability of the membrane toward oxygen. For $\%O_2$ up to 21% (air), good values are $pK'_{SV} = 0.5-1.0$. In order to monitor a wider $\%O_2$ range, $pK'_{SV} = 1.5-2.0$ are good choices. On this basis, an ideal sensor would be prepared with more than one sensing species keeping precision high in all the concentration range. These results may be used also to check the precision of commercial sensors.

Use of $\Delta I_{\%}$ and ASY. Figure 7 reports the two parameters $\Delta I_{\%}$ and ASY as a function of $pK'_{SV} + c$ (where $c = -\log(\%O_2/100)$ and represents a generalization of the curve when $\%O_2 \neq 100\%$ is used). The figure is actually a double working curve in which the model described in the theoretical section may be tested for pK'_{SV} with two parameters simultaneously. In order to check the working curve, in the figure are reported the experimental values of pK'_{SV}, $\Delta I_{\%}$, and ASY obtained from the membrane in Figure 1 (□), that in ref 5 (■) and another nine membranes made by us, characterized by different Ru(dpp)OS concentrations and

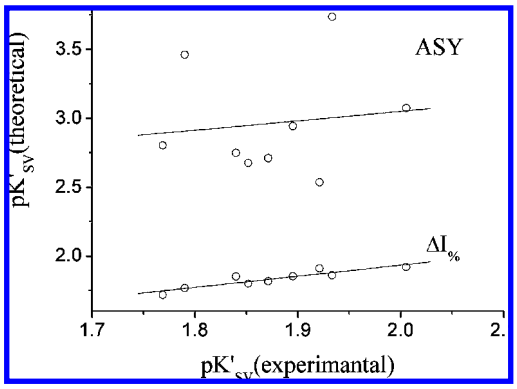

Figure 8. Theoretical vs experimental pK'_{SV} (the former computed with the equation models of pK'_{SV} and $\Delta I_{\%}$ reported in Table 1). Regression parameters of the straight line in the bottom: $y = 0.06(0.14) + 0.94(0.08)x$; $R^2 = 0.98$. Tested membranes characterized by various Ru(dpp)OS concentrations and thicknesses in the range 0.5−10 μm.

thicknesses ranging from 0.5 to 10 μm (○). It is evident that the two membranes represented by the squares at p$K'_{SV} + c = 2.7$ and p$K'_{SV} + c = 0.9$ perfectly overlap the theoretical models (linear Stern−Volmer and only diffusion) as expected. In this case it must be pointed out that the results were obtained with air (%O_2 = 21) so that the two membranes are characterized by pK'_{SV} = 2.0 and pK'_{SV} = 0.2, respectively. The other nine membranes (tested with $c = 0$, %O_2 = 100) are correctly interpreted with the $\Delta I_{\%}$ parameter as all the experimental data well follow the model, while ASY may not be used because the experimental pK'_{SV} values fall in a zone where ASY is insensitive. In fact, ASY is in a low-precision zone so that the pK'_{SV} values estimate is anyway inaccurate as evidenced by the derivatives reported in the inset of Figure 7, which point out a crossing point which indicates that $\Delta I_{\%}$ is more precise for pK'_{SV} > 0.94 and ASY for pK'_{SV} < 0.94 for $c = 0$. The generality of the proposed working curves, given by the "c" constant present in the x-axis, allows to choose the suitable %O_2 value to work in the vicinity of the inflection point, that is, to obtain the most precise value of pK'_{SV}. The reported results are even clearer by considering the graph in Figure 8 representing the experimental pK'_{SV} values vs those computed with ASY and $\Delta I_{\%}$. From that plot it is evident that pK'_{SV} values computed as a function of $\Delta I_{\%}$ correspond to those experimentally determined (p$K'_{SV}(t) = 0.06(0.14) + 0.94(0.08)pK'_{SV}(e)$). The slope and intercept, statistically equal to 1 and 0, respectively, point out the correctness of the chosen model. On the contrary, pK'_{SV} values computed as a function of ASY are dispersed and completely uncorrelated as demonstrated by a t-test. These results state that it is possible to obtain very good values of pK'_{SV} even from only one of the two parameters. A further consideration about ASY is that one or more hypotheses among those reported in the theoretical section may not be true and that they affect only ASY. In the presence of oxygen adsorption, for instance, ASY varied from 15 to 50 while $\Delta I_{\%}$ remained essentially constant (results obtained from data in ref 5).

Estimate of D_{O_2} and s_{O_2}. From the obtained results and from simulation, it is possible to compute the oxygen diffusion coefficient into the membrane from eq 20 and its solubility from eq 13.

$$D_{O_2} = \frac{\gamma_{90}}{t_{90}} L^2 \tag{28}$$

and

$$s_{O_2} = \frac{10^5 K'_{SV}}{4\pi\alpha\sigma N P_{tot} \tau^0 D_{O_2}} \tag{29}$$

The computed values are $D_{O_2} = 2.0 \times 10^{-8}$ cm^2 s^{-1}; s_{O_2}=2.2 × 10^{-3} mol atm^{-1} cm^{-3}. It must be pointed out that the D_{O_2} value needed only the measurement of the membrane thickness, easily obtainable by vis spectroscopy.

CONCLUSIONS

In this paper we pointed out how the sensible parameters $\Delta I_{\%}$ and ASY may be defined from experimental emission data and how they may characterize sensitivity (K'_{SV}) of a generic oxygen optical sensor. The ASY parameter comes from the asymmetric emission shape experimentally observed and is explained with a diffusive model if other phenomena are absent (adsorption, self-quenching, etc.). The correlations between ASY and K'_{SV} and between $\Delta I_{\%}$ and K'_{SV} were established, and a double working curve was proposed to evaluate with a single light emission measurement the K'_{SV} value with the best precision. With this method it has been possible to either characterize the sensitivity of a membrane or plan the construction of a membrane working best in the desired oxygen concentration interval. In fact, very sensitive membranes (pK'_{SV} < 0.5) had very high precision only for low %O_2 values; poorly sensitive membranes (pK'_{SV} > 2.5) had constant precisions, but very low, in a large %O_2 interval. For %O_2 up to 21% (air), good values are pK'_{SV} = 0.5−1.0. In order to monitor a wider %O_2 range, pK'_{SV} = 1.5−2.0 are good choices. Simple mathematical models allowed the estimate of the oxygen diffusion coefficient inside the layer, D_{O_2}, and the oxygen solubility in the polymer matrix, s_{O_2}, from the simple measurement of the membrane thickness, the luminescence lifetime, and membrane response time. $t_{90}D_{O_2} = 2 \times 10^{-8}$ cm^2 s^{-1} and $s_{O_2} = 2.2 \times 10^{-3}$ mol atm^{-1} cm^{-3} were estimated for our membranes. The proposed working curves gave very good results even with the literature data.

ACKNOWLEDGMENT

Funding for this research was provided by the Italian Ministry of University and Research.

Received for review October 25, 2007. Accepted January 8, 2008.

AC702202T